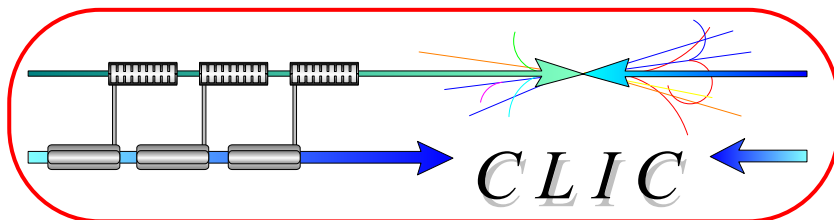


# CERN – EUROPEAN ORGANIZATION FOR NUCLEAR RESEARCH



CLIC Note 513  
PS/AE Note 2002-166  
LCC-Note-0091  
TESLA-2002-08

## TESTS OF 3 LINEAR COLLIDER BEAM DYNAMICS SIMULATION PROGRAMS

D. Schulte, P. Tenenbaum, N. Walker, A. Wolski, M. Woodley

### Abstract

We report on tests of 3 linear collider beam dynamics simulation programs: PLACET, MERLIN, and LIAR. The programs are used to simulate the performance of the TESLA, NLC, and CLIC beamlines from the main linac to the IP. In each case the beamlines have no errors or misalignments.

Geneva, Switzerland  
23rd September, 2002

# Tests of 3 Linear Collider Beam Dynamics Simulation Programs

D. SCHULTE, P. TENENBAUM, N. WALKER, A. WOLSKI, M. WOODLEY  
LCC-NOTE-0091  
TESLA-2002-08  
CLIC-NOTE-513 and CERN PS/AE NOTE 2002-166  
*29-July-2002*

## Abstract

We report on tests of 3 linear collider beam dynamics simulation programs: PLACET, MERLIN, and LIAR. The programs are used to simulate the performance of the TESLA, NLC, and CLIC beamlines from the main linac to the IP. In each case the beamlines have no errors or misalignments.

## 1 Introduction

In the context of the International Linear Collider Technical Review Committee (ILC-TRC), it is necessary to review the performance of tuning algorithms and diagnostic devices for TESLA, NLC, and CLIC in order to evaluate the reliability of their published luminosity estimates. The most straightforward means of reviewing such algorithms is to implement each one in simulation and observe the results.

Three simulation programs are available to the TRC which are deemed adequate in principle for use in this context: PLACET [1]; MERLIN [2]; and LIAR with DIMAD tracking options [3, 4]. One pre-requisite for establishing confidence in the results of the tuning simulations is to ensure that each program is reliably simulating the basic beam dynamics of the linear colliders.

To this end, we simulated CLIC, NLC, and TESLA main linac and beam delivery regions using all 3 of the aforementioned programs. The simulations were for “perfect” machines: no misalignments or errors were present. In addition, the TESLA and NLC bunch compressor systems were simulated using MERLIN, LIAR, and MAD [5].

## 2 Basic Physics and Parameters of Interest

The tests concentrated on a limited group of studies that were expected to reveal any deviations between the programs which would be significant during the tuning studies. These tests are described below.

### 2.1 Bunch Compressors

The fundamental quantities of interest in the bunch compressor studies are:

- Final RMS bunch length
- Final RMS energy spread
- Final centroid energy

Note that the NLC bunch compressor was simulated with longitudinal and transverse wakefields, while the TESLA bunch compressor was simulated without wakefields. Because of the details of the TESLA bunch compressor design, the wake-free case is believed to be a reasonable simulation of the system for perfect machine studies.

## 2.2 Accelerator Structures

Because of the overwhelming importance of linear accelerating structures to each main linac, the simulation of individual accelerating structures was performed. In one case, a TESLA bunch compressor structure with a pitch angle misalignment was simulated, to ensure that the resulting coupling of the fundamental mode into the transverse was properly modelled. In another case, an NLC main linac structure with a transverse offset misalignment was simulated, to ensure that transverse wakefields were properly modelled.

## 2.3 Main Linacs

Each main linac was simulated under 2 conditions: with an on-axis, nominal bunch, and with a nominal bunch offset by  $1 \sigma_y$  at injection. The parameters of interest are:

- Normalized emittance growth at extraction, both cases
- Centroid energy and RMS energy spread, on-axis case
- Normalized vertical emittance growth along the linac, off-axis case.

## 2.4 Main Linac to Interaction Point

Each ensemble of main linac and beam delivery system was tested under the same 2 conditions used for the main linac. Parameters of interest are:

- RMS beam size at IP, both cases
- Centroid position at IP, both cases
- Normalized emittance growth at IP, both cases

Finally, for each design the bandwidth of the beam delivery system was measured. This was done by generating a beam with a very small energy spread and measuring the RMS beam size and position at the IP as a function of centroid energy. It is important to note that the resulting “bandwidth” is not a useful measure of the real-world performance of anything, but merely a useful tool to ensure that the simulation codes are in adequate agreement for beams which are far from the nominal energy.

# 3 Brief Description of the Simulation Codes

Please note that in the following descriptions, the words “cavity” and “structure” should be treated as synonymous; both words refer to a multi-cell linear accelerating element.

## 3.1 LIAR

LIAR uses two different tracking engines for different parts of the study. For linacs, bunch compressor RF structures, and other simple transport lines, the beam is represented as “macroparticles;” each macroparticle has associated with it a charge, a vector of 6 centroid positions, and a matrix of 10 second moments (in the transverse plane). The full 6-dimensional beam is represented by a series of macroparticles, each of which has a distinct energy and z position (note that macroparticles are monoenergetic and have no longitudinal extent). Acceleration is modelled directly – all macroparticles have as the sixth component of the first moment vector an energy  $E$  in GeV. RF

structure matrices (including end focusing) and quad matrices are calculated to first order, but are calculated for each macroparticle according to its energy and the parameters of the structure or quad. Wakefields are applied as an impulse at the center of each structure. Calculations were performed with 11 macroparticles per longitudinal position, 51 longitudinal positions per beam, with truncation at  $\pm 3\sigma_z$ ; energy truncation of the initial distribution is also truncated at  $\pm 3\sigma$ . For beamlines with momentum compaction or multipoles above quadrupole, the beam is converted to dimensionless rays (typically 80 to 100 rays per LIAR macroparticle) which are tracked through  $R$ - and  $T$ - matrices. The matrices are calculated statically as an expansion about the design energy (ie, if the design energy is 250 GeV and the beam energy centroid is 249 GeV, the quad matrices are calculated at 250 GeV). Rays are generated to  $\pm 5\sigma$  in transverse planes.

### 3.2 MERLIN

Merlin performs particle tracking using first- and second-order TRANSPORT matrices [6] for drifts and all multipoles up to and including sextupole. Higher- order multipoles are treated as thin-lens kicks at the centre of a drift. The maps are expanded about the current reference energy at that element. Acceleration is modelled as an increase in the reference energy and a corresponding adjustment of the individual particle  $\Delta p/p$  to reflect the curvature of the RF. In the transverse plane, cavities are modelled as a linear matrix which includes the cavity end focusing. Wakefield effects are applied as an impulse at the exit of each cavity. Particles are binned longitudinally in 100 slices over  $\pm 3\sigma_z$  to estimate the charge distribution, from which the bunch wakefields are estimated. The wakefield kicks are calculated for each particle using linear interpolation of the resulting bunch wakefield table. The initial random coordinates were generated from a Gaussian distributions in all six dimensions, truncated at  $\pm 5\sigma$  in the transverse planes and  $\pm 3\sigma$  in the longitudinal plane. For the BDS bandwidth studies,  $10^3$  particles were tracked, using the same truncation. For the bunch compressor and linac to IP studies – where wakefields are included –  $10^4$  particles were tracked.

### 3.3 PLACET

In PLACET, the beam can be represented by rays, each of which is described by a 6-dimensional vector containing its position, transverse angles, and energy. Also a weight factor is attributed to each particle. To efficiently simulate linear systems, also a macroparticle representation can be used. In this case each beam is represented by slices, which in addition to the position vector also contain 10 second moments.

Tracking in quadrupoles and structures is performed by applying the first order matrices, which are calculated for each particle's energy separately. In the structures the wakefield kick is applied as an impulse in the center, and the structure end fields are taken into account. The wakefield calculation is performed by cutting the beam longitudinally into slices. Multipoles higher than the quadrupole are modelled by using a series of thin lenses. For the present simulations, five thin lenses are used for all elements which have a non-zero length. The matrix for each lens is calculated for each particle separately. For each quadrupole, bend, and multipole one can choose to include synchrotron radiation.

For all simulations 40,000 particles were used, distributed over 51 slices. No cut in transverse initial position, angle, or energy was applied; only the longitudinal position in the beam was limited to  $|z| \leq 3\sigma_z$ . Synchrotron Radiation was switched off in all elements.

Since PLACET does not at present simulate momentum compaction, any element with significant momentum compaction is simulated using the program MAD [5]. An interface routine has been developed to allow a smooth transition between elements simulated by PLACET and elements simulated by MAD.

## 4 Results of Simulation Tests

### 4.1 Bunch Compressors

Table 1 shows the input conditions used for the 2 bunch compressor designs and the design output parameters. Note that the NLC bunch compressor includes a 6 GeV linac, which is why the extraction energy is so much higher than the injection energy. Table 1 also shows the results of bunch compressor simulations for the various programs.

Table 1: Parameters and Results of Bunch Compressor Simulations. No MAD studies of the NLC bunch compressor were performed.

Parameter	Unit	Program	TESLA	NLC
$\sigma_z$ Initial	mm	All	6.0	5.0
$\sigma_\delta$ Initial	%	All	0.13	0.1
$E$ Initial	GeV	All	5.00	1.98
$\sigma_z$ Final	mm	Design	0.300	0.110
		MAD	0.290	
		MERLIN	0.287	0.106
		LIAR	0.284	0.109
$\sigma_\delta$ Final	%	Design	2.80	1.40
		MAD	3.12	
		MERLIN	3.10	1.31
		LIAR	3.18	1.48
$E$ Final	GeV	Design	4.600	7.870
		MAD	4.593	
		MERLIN	4.594	7.887
		LIAR	4.596	7.882

### 4.2 Accelerator Structure Tests

A pitched or yawed accelerator structure imparts a time-varying transverse kick to a bunch which passes through it. In this test, a TESLA bunch compressor structure and a damped, uncompressed TESLA beam were used and the kick angle versus  $z$  was measured. Critical parameters include: the structure frequency (1.3 GHz), length (1.036 meters), on-crest, unloaded energy gain (20.25 MeV), phase ( $-115^\circ$ ), and pitch angle (1 mrad); the RMS bunch length (6 mm) and centroid energy (5 GeV). The bunch was simulated with the TESLA damping ring energy spread of 0.13%, but this was found to have an immeasurably small effect. Figure 1 shows the deflection as a function of  $z$  along the bunch, taking the convention that  $z < 0$  is the bunch head and  $z > 0$  is the tail. This is the convention used by LIAR and DIMAD; MERLIN and MAD take the opposite convention, and PLACET...?. Where necessary, native program conventions have been adjusted to produce data adequate for comparison in Figure 1.

An accelerator structure with an offset causes a deflection to the bunch which varies in  $z$  due to the buildup of wakefields. In this test, an NLC structure and a compressed NLC beam were used and the kick angle versus  $z$  was measured. Critical parameters include: the structure wake per unit length (the standard NLC wake was used), length (0.9075 m), on-crest unloaded energy gain (zero), and offset (1 mm); the bunch RMS length (110  $\mu\text{m}$ ), charge ( $0.75 \times 10^{10}$ ), and centroid

energy (7.87 GeV). Figure 2 shows the deflection angle along the bunch, with the same head-tail convention as was used in Figure 1.

### 4.3 Main Linacs

Table 2 lists the initial conditions, design results, and simulation results of the main linac study. All beams were generated with Gaussian distributions in all degrees of freedom, and the correlation between longitudinal position and energy within the bunch was assumed to be zero. For on-axis beams, emittance growth was very close to zero in all cases, and is not reported here.

Table 2: Parameters and results of main linac simulations.

Parameter	Unit	Program	TESLA	NLC	CLIC
$\beta_x$	m	All	92.7889	23.107	6.6868
$\beta_y$	m	All	47.5810	2.8782	2.7269
$\alpha_x$	–	All	-1.6154	-2.7952	-1.7211
$\alpha_y$	–	All	0.6969	0.4024	0.7851
Energy	GeV	All	4.60	7.87	9.0
$\sigma_\delta$	%	All	3.00	1.40	2.0
$\sigma_z$	mm	All	0.300	0.110	0.035
Charge	$10^{10} e$	All	2.0	0.75	0.4
$\gamma\epsilon_x$	$\mu\text{m}$	All	8.0	3.0	1.8
$\gamma\epsilon_y$	nm	All	20.0	20.0	5.0
End Energy	GeV	Design	250.0	250.0	250.0
		PLACET	251.280	249.997	249.63
		MERLIN	251.300	249.928	250.01
		LIAR	251.282	249.941	250.0
End Energy Spread	%	Design	0.075	0.25	0.25
		PLACET	0.077	0.302	0.257
		MERLIN	0.078	0.292	0.250
		LIAR	0.076	0.288	0.256
$\Delta\gamma\epsilon_y, 1\sigma_y$ Initial Offset	nm	PLACET	4.09	8.75	3.65
		MERLIN	4.28	8.82	3.69
		LIAR	4.44	8.66	3.53

Figure 3 shows the normalized emittance growth down the linac for a  $1\sigma_y$  beam offset at injection.

### 4.4 Main Linac to IP Tests

The tests of full system from main linac to IP used the same initial parameters reported in Table 2 for the main linac studies. The results are shown in Table 3. Note that the “horizontal emittance growth” reported for the NLC and CLIC cases includes the contribution from the  $\eta'_x$ , and is therefore not indicative of the amount of true horizontal emittance growth.

Table 3: Parameters and results of main linac to IP simulations. Note that the beam vertical position at the IP is on the order of 1% of the RMS beam size, which is the statistical resolution limit of the simulation as performed.

Parameter	Unit	Program	TESLA	NLC	CLIC
$\sigma_x^*$	nm	PLACET	490	223	197
		MERLIN	505	223	198
		LIAR	504	223	190
$\sigma_y^*$	nm	PLACET	4.22	2.27	1.44
		MERLIN	4.28	2.26	1.36
		LIAR	4.21	2.28	1.46
$x^*$	nm	PLACET	30.7	-28	-55
		MERLIN	35.2	-18.8	-34
		LIAR	30.4	-22.4	-37.1
$y^*$	pm	PLACET	1	-44	15
		MERLIN	-1.0	-87	41
		LIAR	-5.4	-5.18	-3.9
$\Delta\gamma\epsilon_x$	$\mu\text{m}$	PLACET	0.14	1.39	0.89
		MERLIN	0.19	1.34	0.90
		LIAR	0.21	1.39	0.86
$\Delta\gamma\epsilon_y$	nm	PLACET	0.53	0.95	1.05
		MERLIN	0.5	0.76	0.90
		LIAR	0.2	0.98	1.22
$\sigma_y^*$ $1\sigma_y$ Initial Offset	nm	PLACET	4.70	2.75	2.13
		MERLIN	4.71	2.64	3.18
		LIAR	4.68	2.71	4.84
$\Delta\gamma\epsilon_y$ $1\sigma_y$ Initial Offset	nm	PLACET	8.1	10.3	7.4
		MERLIN	8.2	10.0	14.8
		LIAR	7.8	10.3	25.1

## 4.5 Beam Delivery System Bandwidth Study

The beam delivery systems of the 3 linear colliders were studied with incoming beams of different energies. Table 4 shows the parameters used at the entrance to the various systems. In the case of the NLC, the beamline included the bypass line and its injection and extraction regions (i.e. all of the NLC downstream of the *BEGELTB* marker). For TESLA, the *EBDS* line was used, and for CLIC the (*MYCOLLSYS, EFF1S*) line was used.

Table 4: Initial conditions for BDS Bandwidth study.

Parameter	Unit	TESLA	NLC	CLIC
$\beta_x$	m	156.76	62.902	8.5786
$\beta_y$	m	78.697	12.398	28.1491
$\alpha_x$	–	1.5835	2.2699	0.6318
$\alpha_y$	–	-0.8797	-0.5123	-1.8976
Min Energy	GeV	247.5	247.5	247.5
Max Energy	GeV	252.5	252.5	252.5
$\sigma_\delta$	%	0.0001	0.0001	0.0001
$\sigma_z$	mm	0.300	0.110	0.035
Charge	$10^{10} e$	2.0	0.75	0.4
$\gamma\epsilon_x$	$\mu\text{m}$	8.0	3.0	2.0
$\gamma\epsilon_y$	nm	20.0	20.0	20.0

Figures 4, 5, and 6 show the results of the studies for TESLA, NLC, and CLIC, respectively.

## 5 Conclusion

Three programs used for the simulation of linear collider beam transport have been compared to one another. In general, the programs show excellent agreement on the parameters studied.

In a few cases, the agreement is not yet good enough, and in these cases more effort should be invested in resolving the discrepancies. The specific areas of remaining concern are: the linac-to-IP vertical emittance growth for on-axis beams; the beam size and vertical emittance growth for  $1 \sigma_y$  oscillation through linac and BDS, in the case of CLIC; the NLC and CLIC  $y^*$  for off-energy beams; and the TESLA BDS bandwidth. Of these, the last is of greatest concern, since TESLA contains a fascinating set of interleaved normal and skew multipole elements, and the performance of such a system must be independently and multiply verified.

## References

- [1] E.T. d’Amico, G. Guignard, N. Leros, D. Schulte, “Simulation Package Based on PLACET,” Proceedings of the 2001 Particle Accelerator Conference (2001).
- [2] <http://www.desy.de/~merlin>.
- [3] R. Assmann *et al*, “The Computer Program LIAR for the Simulation and Modeling of High Performance Linacs,” Proceedings of the 1997 Particle Accelerator Conference (1997).



- [4] P. Tenenbaum, L. Hendrickson, A. Seryi, G. Stupakov, “Recent Developments in the LIAR Simulation Code,” to be published in Proceedings of the 2002 European Particle Accelerator Conference (2002).
- [5] H. Grote, F.C. Iselin, “The MAD Program Users’ Reference,” CERN-SL-90-13 (AP) Rev 5 (1996).
- [6] D.C. Carey, K.L. Brown, F. Rothacker, “Third-Order TRANSPORT, a Computer Program for Designing Charged Particle Beam Transport Systems,” SLAC-R-462 (1995).

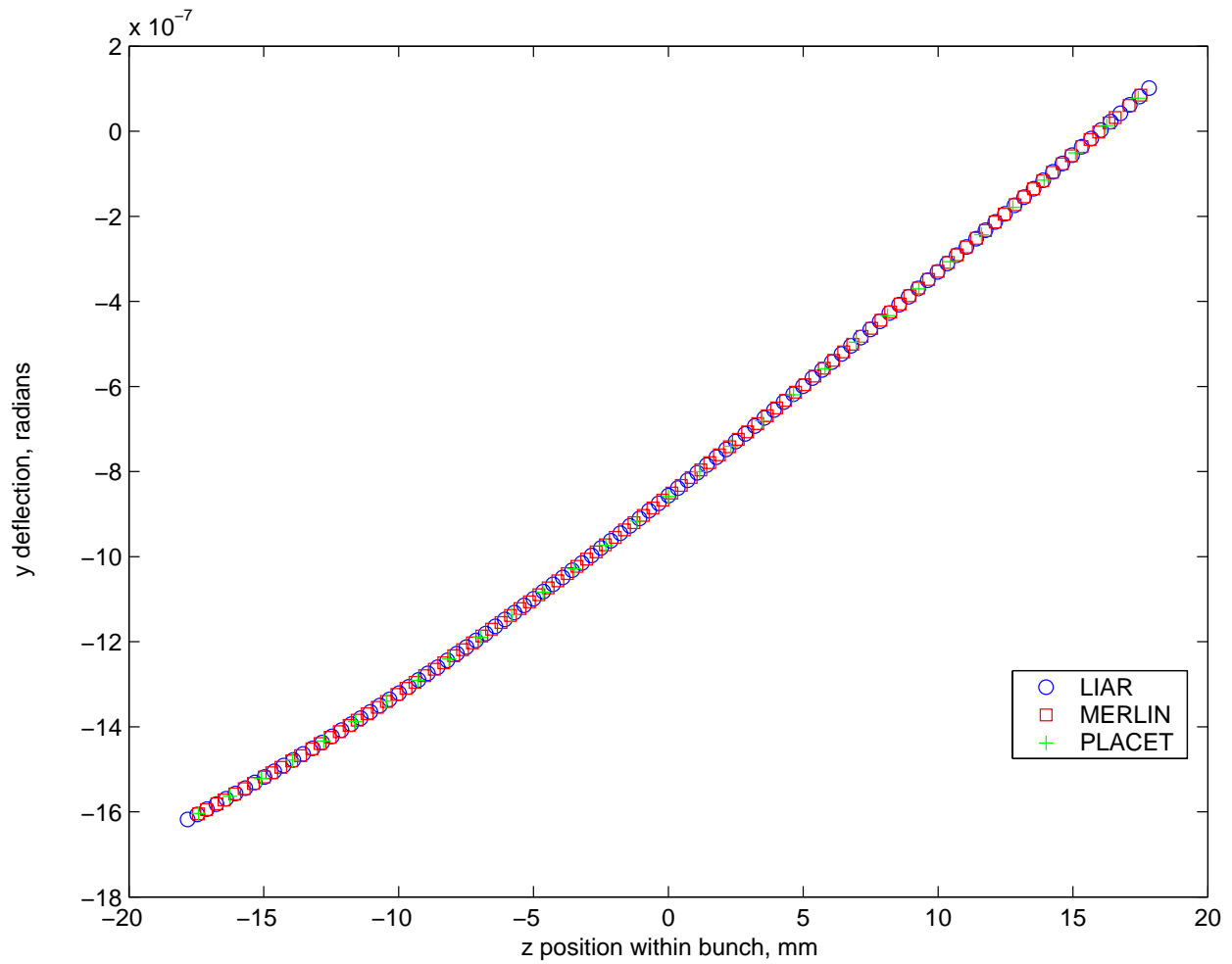


Figure 1: Deflection along a bunch due to a tilted TESLA structure.

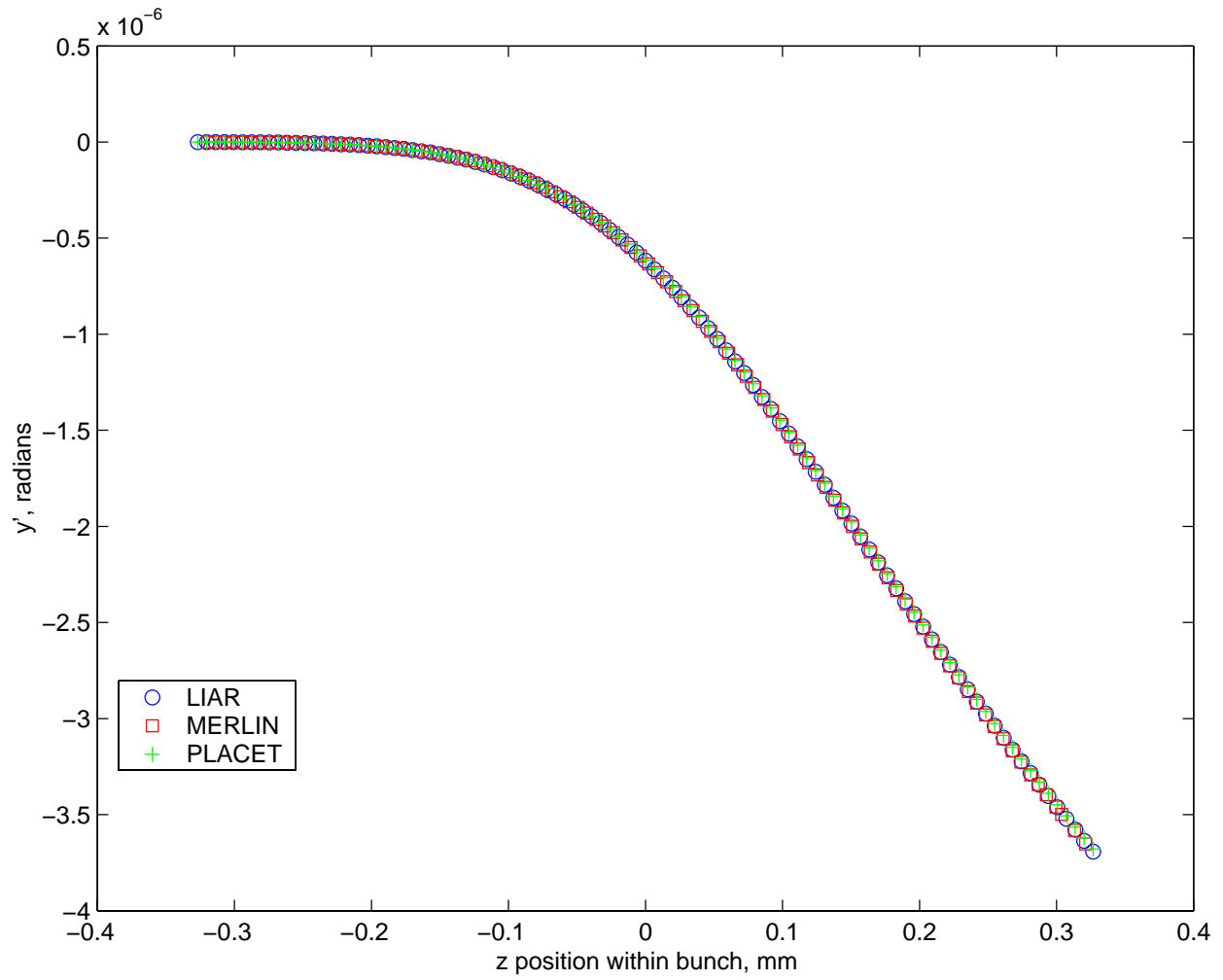


Figure 2: Deflection along a bunch due to an offset NLC structure.

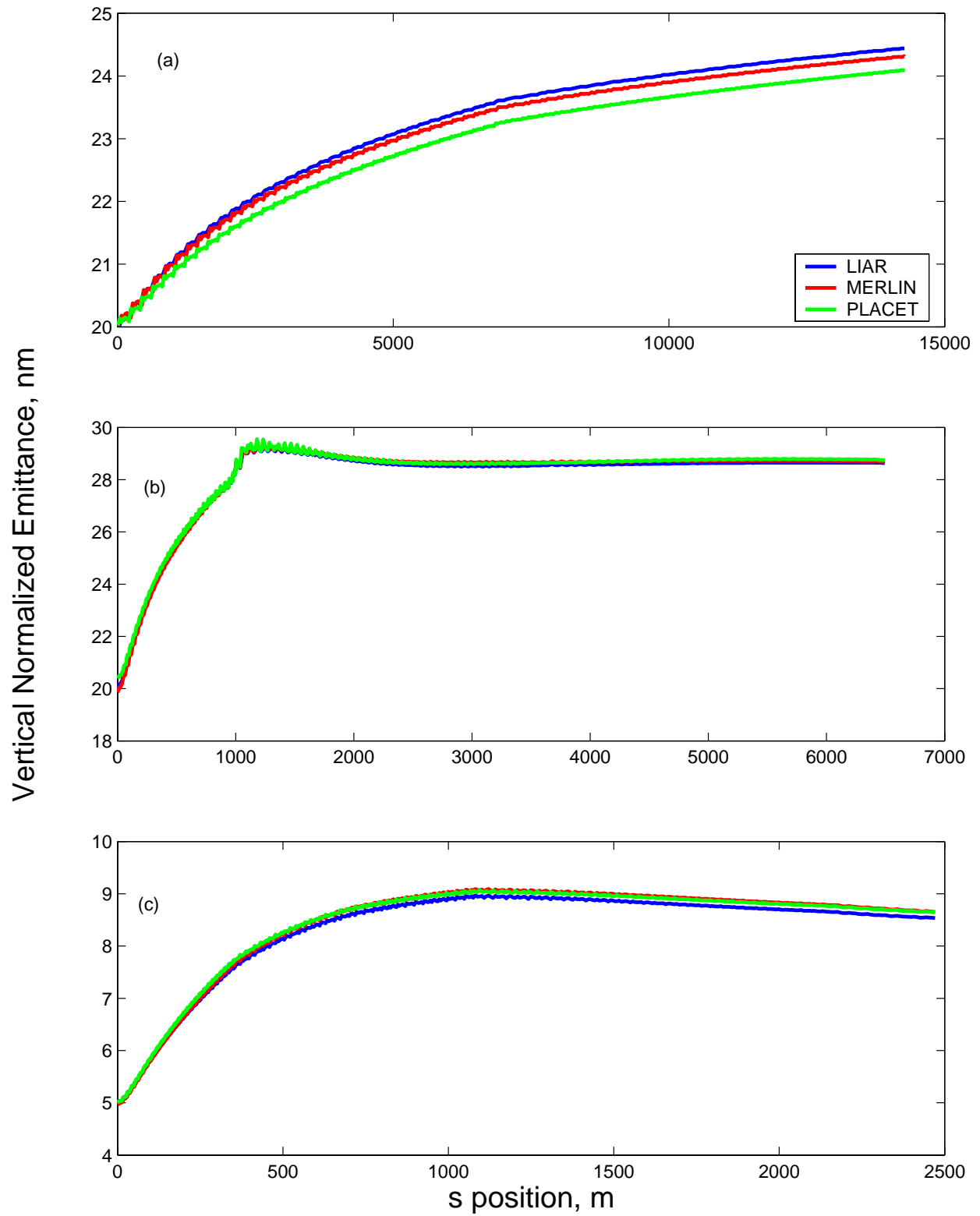


Figure 3: Emittance growth due to  $1 \sigma_y$  beam offset at injection: (a) TESLA (b) NLC (c) CLIC.

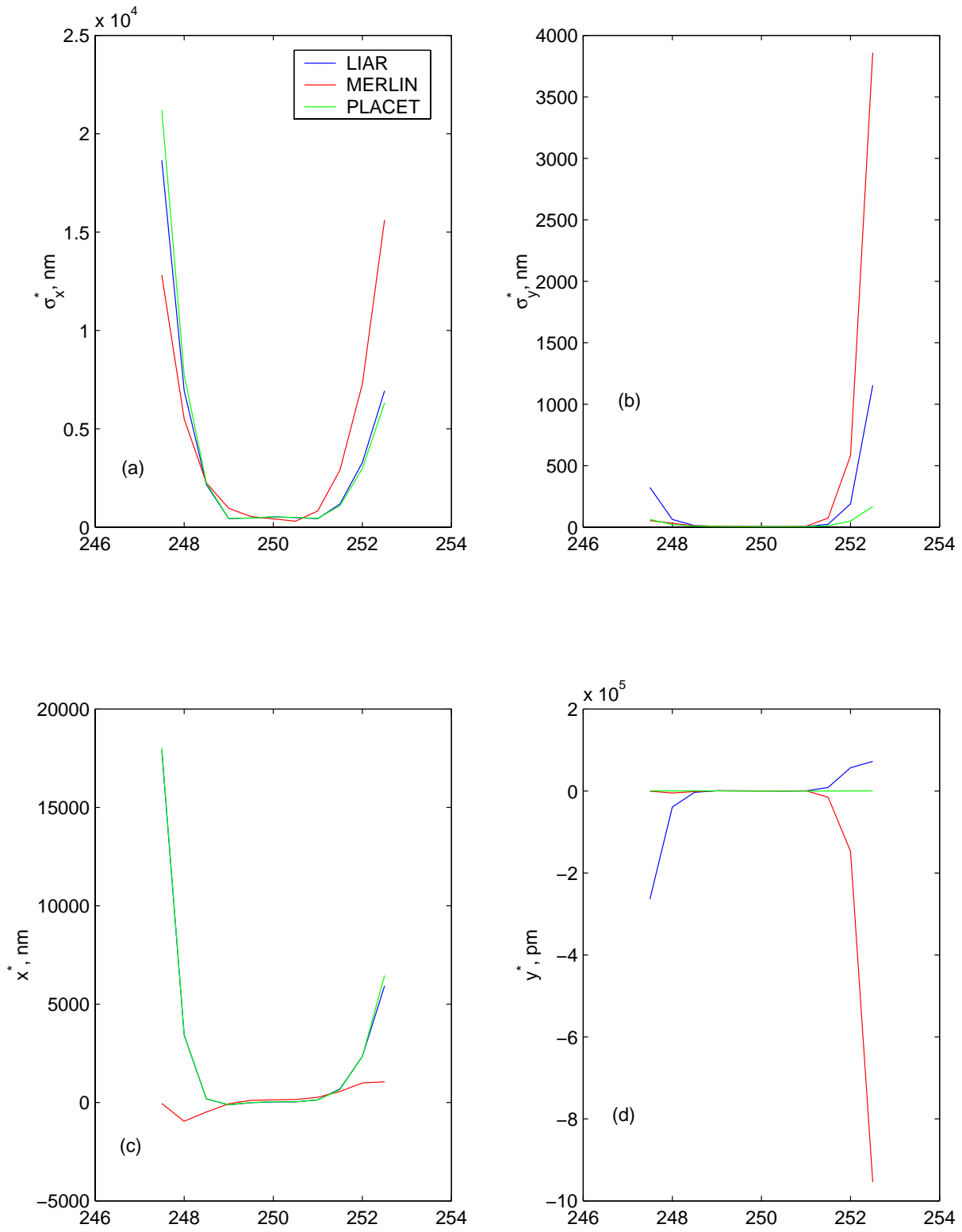


Figure 4: Performance of the TESLA BDS for monochromatic beam, as a function of injection energy in GeV: (a)  $\sigma_x^*$ , (b)  $\sigma_y^*$ , (c)  $x^*$ , (d)  $y^*$ . All values are in nm except for (d), which is in pm.

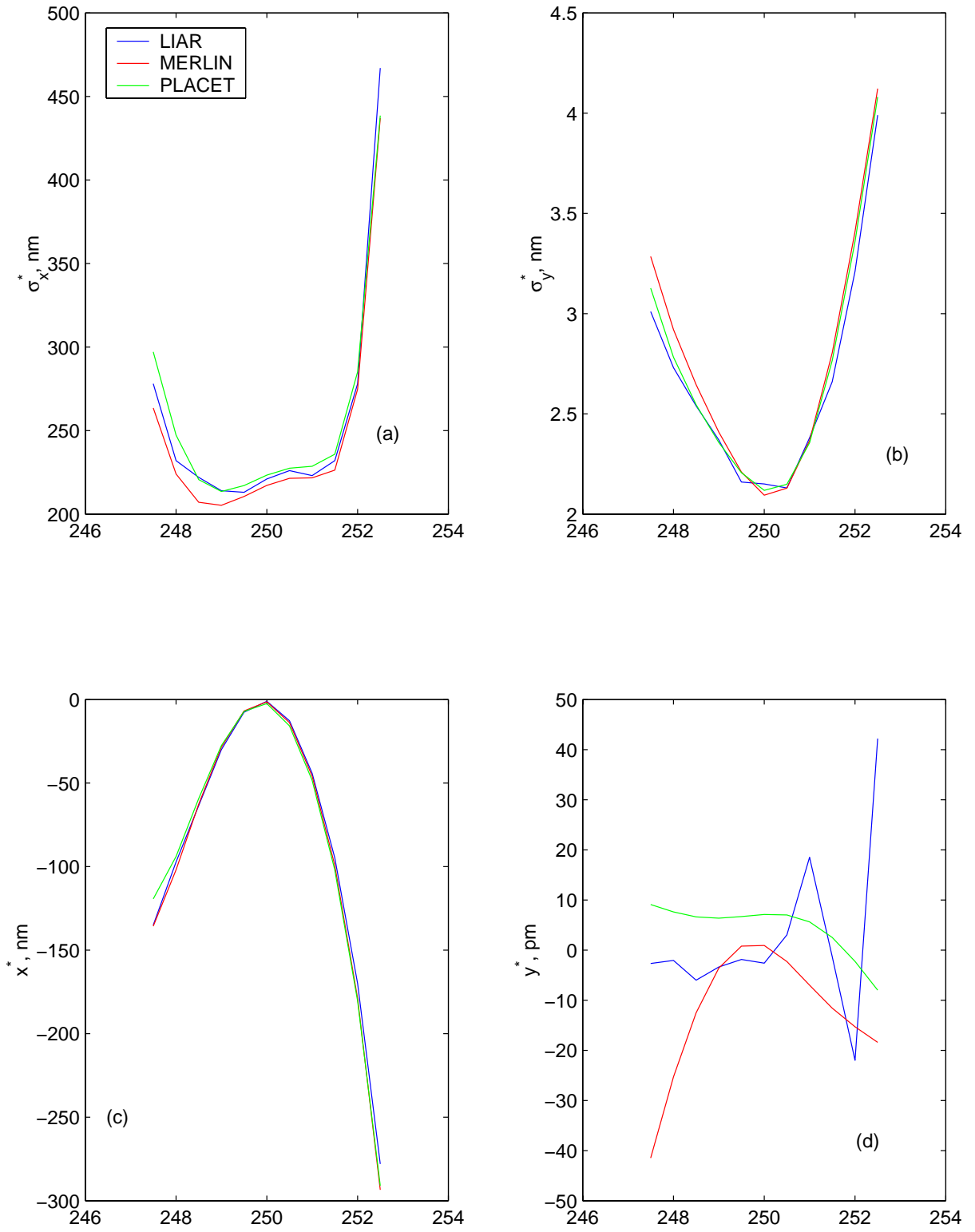


Figure 5: Performance of the NLC BDS for monochromatic beam, as a function of injection energy in GeV: (a)  $\sigma_x^*$ , (b)  $\sigma_y^*$ , (c)  $x^*$ , (d)  $y^*$ . All values are in nm except for (d), which is in pm.

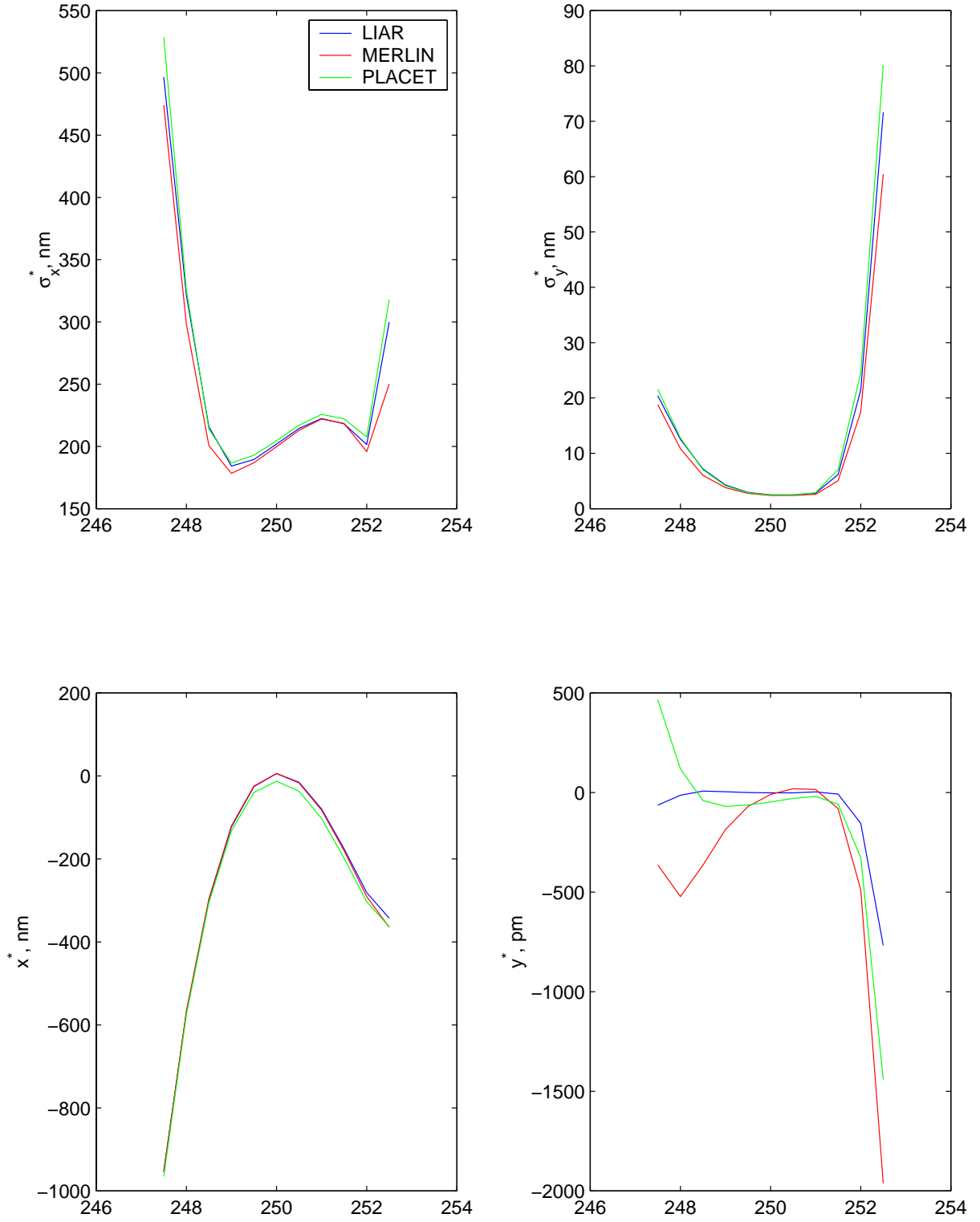


Figure 6: Performance of the CLIC BDS for monochromatic beam, as a function of injection energy in GeV: (a)  $\sigma_x^*$ , (b)  $\sigma_y^*$ , (c)  $x^*$ , (d)  $y^*$ . All values are in nm except for (d), which is in pm.